JLAB-TN-03-015
28 April 2003

Performance Qualification of 2F Region GX/GQ Dipoles

G. Biallas, D. Douglas, T. Hiatt, and *C. Tennant*

Abstract

We document the observed performance of IR FEL Upgrade GX and GQ magnets intended for use in the first recirculation arc, and compare it to specification.

Performance Criteria

IR FEL Upgrade dipoles are to comply with the design and performance specifications [1] given below. We note that the following criteria represent requirements that have been relaxed relative to earlier specifications [2] inasmuch as we will qualify the magnets based on performance at 80 MeV/c and 145 MeV/c only, rather than on the originally intended 80 MeV/c to 210 MeV/c operating range. Schedule, schedule, schedule, schedule, ….

Performance Criteria

1. At operating currents I_{145} and I_{80} appropriate respectively to each of 145 MeV/c and 80 MeV/c, verify the core field agrees with design to within 1‰. This guarantees the beam will bend on the correct radius to within error tolerances.
2. At the same operating currents, verify the field integral along the central orbit agrees with design to within 1‰. This guarantees the beam will bend through the correct angle to within error tolerances.
3. At the same operating currents, certify the field integral along the DIMAD chord, the half sagitta line, and the tangent cord agree with design to within 0.1‰. This guarantees the dipole "wedge angle", and thus the focusing applied to the beam, are correct to within error tolerances.
4. At the same operating currents, verify the contour maps of the field are not pathological and that they indicate that the field variation transverse to the design orbit is at the 0.1‰ level across the working aperture (4 cm + $6\sigma_{betatron} + \eta\ \delta p/p$). This certifies that phase space distortion will be avoided
5. At the same operating currents, verify the field variation transverse to the design orbit is at the 0.1‰ level across the working aperture (4 cm + $6\sigma_{betatron} + \eta\ \delta p/p$), again certifying that phase space distortion will be avoided.

In the following, we will take β~5 m, ε_N~30 mm-mrad, E ~80 MeV, implying $\gamma=E/mc^2$~150, η_{GX}~0.33 m, η_{GQ}~1.7 m, and $\delta p/p$ ~0.1 to get a working aperture requirement (around the reference orbit) of ~10 cm in the GX and 22 cm in the GQ.

Observed Performance of Dipoles to be used in the First Arc

GQ001, GQ002, GX001, GX002, and GX003 have been measured as documented elsewhere [3]. GX002 was observed to have a leaky coil, and will therefore be replaced in the first arc (3F region) by GX003. After repair, it will be used in the second arc (5F region). The following information thus serves to qualify GQ001, GQ002, GX001 and GX003 for use in the 3F region. Data pedigrees are as follows:

GQ001: Hiatt e-mail of 2/7/2003, files 145mev~1.xls & 80mevg~2.xls
GQ002: Hiatt e-mail of 1/27/2003, files 145MEV~1.XLS & 80MEVG~1.XLS
GX001: Hiatt e-mail of 1/28/2003, files 145MEV~2.XLS & 80MEVG~1.XLS
GX003: Hiatt e-mail of 2/03/2003, files 145MEV~1.XLS & 80MEVG~1.XLS

<u>Criterion 1</u>: Table 1 presents design and measured values for core field in each dipole at 145 and 80 MeV/c. The design value is established using $B=(B\rho)/\rho=33.3564\ p/\rho$ [kg], with p in GeV/c and ρ =1.2 m. The "measured value" is established by peering at the raw data and picking a nice looking value – one that seems to appear within "most" of the magnet. The operating current was selected to allow for enhancement of the measured field (which is observed without the beam vacuum chamber in place) by the vacuum chamber; this effect scales the field by about 0.2%. Thus, the relevant observable is the field seen by the beam, or the "chamber corrected" field $B_{corrected}=1.002 \times B_{measured}$. The deviation is defined as $(B_{corrected}- B_{design})/B_{design}$.

Table 1: Design and Observed Core Field Values

	GQ001	GQ002	GX001	GX003
B_{design}(145 MeV/c) (g):	4030.56	4030.56	4030.56	4030.56
I_{145} (A)	153.64	153.64	153.64	153.64
$B_{measured}$(145 MeV/c) (g): Chamber corrected (g):	4022 4030	4022 4030	4024 4032	4022.5 4030.5
ΔB/B	-0.00014	-0.00014	0.00036	-0.000015
B_{design}(80 MeV/c) (g):	2223.76	2223.76	2223.76	2223.76
I_{80} (A)	84.79	84.79	84.79	84.79
$B_{measured}$(80 MeV/c) (g): Chamber corrected (g):	2228.5 2233.0	2228 2232.5	2230 2234.5	2228.5 2233.0
ΔB/B	0.0042	0.0039	0.0048	0.0042

We observe that all magnets meet specification at 145 MeV/c, and at 80 MeV/c all magnets deviate from specification by offsets that are systematic (with a value of ~0.004) to within the variation tolerance of 1‰. Thus (provided the GY shunt has adequate range) the core field can be systematically migrated to the required value of ~2224 by a 4‰ change of the 2F dipole buss. The core fields therefore can be made to track amongst the various magnets and families to within specification. In subsequent sections we will determine if (actually, *that*) field integrals similarly track.

Criterion 2: Table 2 presents field integrals along the reference orbit for each magnet at both 145 and 80 MeV/c. The design field integral is simply (Bρ)θ, with Bρ=33.3564 p [kg-m]; θ=43.383565^{o} and, as above, p is in GeV/c. the observed integrals along the reference orbit were independently evaluated using Igor and Excel. Figure 1 illustrates the reference orbit geometry and the range of measured data in relation to the magnet poles for both GX and GQ. We note the data was taken over a smaller region than that influenced by fringe field of the magnet so that truncation errors are present. The excluded field integral was due to fields of order 1 g over a few tens of cm, and thus amounts to an error of order a few 10s of g-cm, or 0.1‰ in the results. This is well below the specified 1‰ tolerance. We have similarly ignored the effect of the earth's field in this evaluation, to similar effect. We have, however, included chamber compensation – a factor of 1.002 representing the effect of the vacuum chamber, which was not present during magnetic measurement. The relative deviations, calculated as $\Delta BL/BL=(\int B_{corrected}dl-(B\rho)\theta)/(B\rho)\theta$, are calculated using the corrected integral.

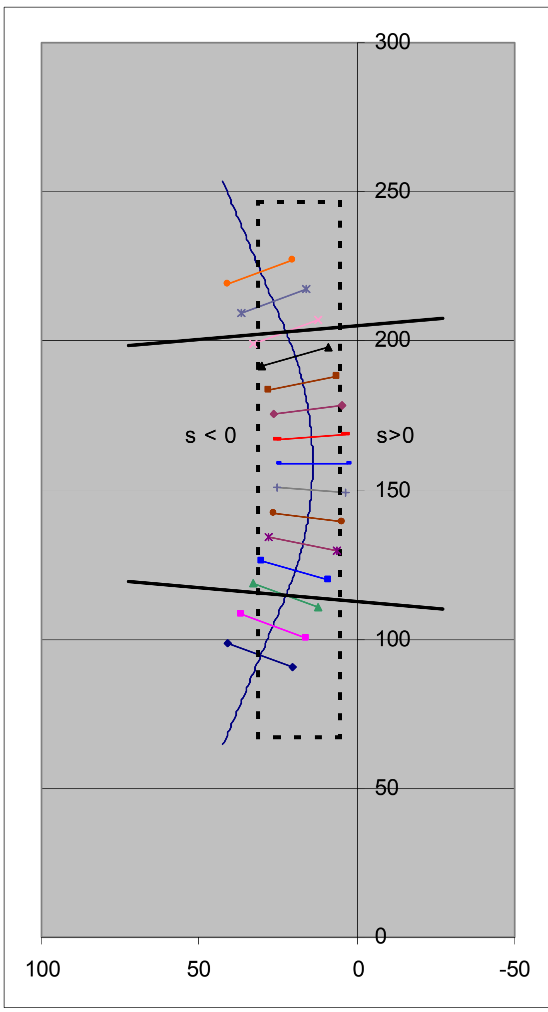

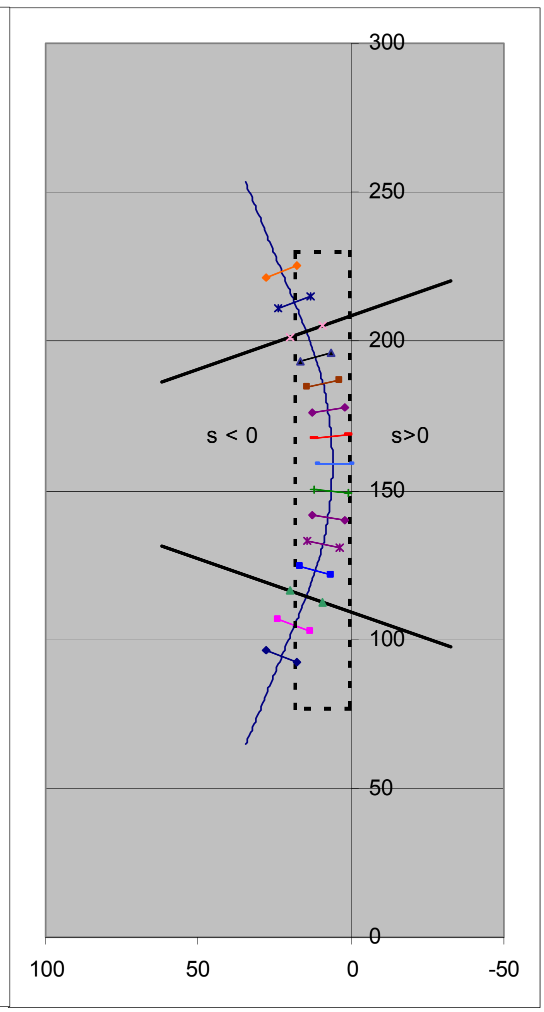

Figure 1 – GQ (left) and GX (right) measurement, reference orbit, and transverse cut geometry

We also include an entry for $B_{core}\rho\theta$ (with $\rho = \rho_{design}$= 120 cm and θ as above), to provide an additional figure of comparison. Intuitively, a well behaved or nearly ideal magnet with uniform core field will provide a field integral equal to the core field times the path length, or ρθ. This must also undergo correction to account for the effect of the vacuum chamber (which scales the field by 1.002). The deviation of the chamber corrected estimate from design, $\delta BL/BL=(1.002\times B_{core}\rho\theta- (B\rho)\theta)/(B\rho)\theta$, is given as well.

Table 2: Field integrals along reference orbit.

	GQ001	GQ002	GX001	GX003
(Bρ)θ (g-cm, @145 MeV/c)	366227	366227	366227	366227
∫Bdl (g-cm, @145 MeV/c): Igor Excel	362736 362467	365628 365316	365101 365062	364835 364852
Chamber Corrected: Igor Excel	363461 363192	366359 366047	365831 365792	365565 365582
ΔBL/BL @ 145 MeV/c: Igor Excel	-0.0076 -0.0083	0.00036 -0.00049	-0.0011 -0.0012	-0.0018 -0.0018
$B_{core}\rho\theta$ (g-cm, @145 MeV/c)	365448	365448	365630	365494
Chamber Corrected	366175	366175	366361	366224
δBL/BL @ 145 MeV/c	-0.00014	-0.00014	0.00037	-0.00001
(Bρ)θ (g-cm, @80 MeV/c)	202056	202056	202056	202056
∫Bdl (g-cm, @80 MeV/c): Igor Excel	201040 200932	202514 202568	202215 202438	202131 202290
Chamber Corrected: Igor Excel	201442 201334	202919 202973	202619 202843	202535 202695
ΔBL/BL @ 80 MeV/c: Igor Excel	-0.0030 -0.0036	0.0043 0.0045	0.0028 0.0039	0.0024 0.0032
$B_{core}\rho\theta$ (g-cm, @80 MeV/c)	202487	202441	202623	202487
Chamber Corrected	202892	202846	203028	202892
δBL/BL @ 80 MeV/c	0.0041	0.0039	0.0048	0.0041

These data suggest that GX001, GX003, and GQ002 track not only in core field (Criterion 1), but in integral as well. GQ001 tracks in core field, as indicated in Table 1 and the B_{core} ρθ data of Table 2, but not in integral. This is because GQ001 was not shimmed prior to the measurements from which data are presented here, but GQ002 was. We note that the field integral (or, equivalently, the effective length) decrement tracks from 145 MeV/c to 80 MeV/c. At 145 MeV/c the three "good" magnets all exhibit correct (to within specification) field and field integral. At 80 MeV/c, all three exhibit field and integral that are ~0.4% high. At 145 MeV/c, GQ001 has the correct field, but the integral is ¾% low; at 80 MeV/c this magnet provides field that is 0.4% high (just like the other three) but the integral is ~1/3% below design – or, in other words ~¾%

below that of the other three. We therefore expect that when GQ001 is shimmed in the same manner as was GQ002, it will behave similarly, providing field and integral to within specification at 145 MeV/c and systematically providing field and integral that are too strong by 0.4% at 80 MeV/c. As both core field and integral for all four magnets will then track, the excitation error at 80 MeV/c can be compensated by shifting the arc dipole buss and compensating the GY with its shunt (assuming there is adequate shunt range).

Criterion 3: Inspection of Figure 2 shows that Criterion 3 may not be met for GX magnets, but should be for GQ. This is a modification of Figure 1, in which the design orbit and the limits of the working aperture (dashed blue lines) are shown superposed on the magnet poles (solid black lines) and the measurement range (dashed black lines). The red lines show the integration paths under discussion; the dashed indicate the DIMAD and tangent chords, the solid lies along the half-sagitta line.

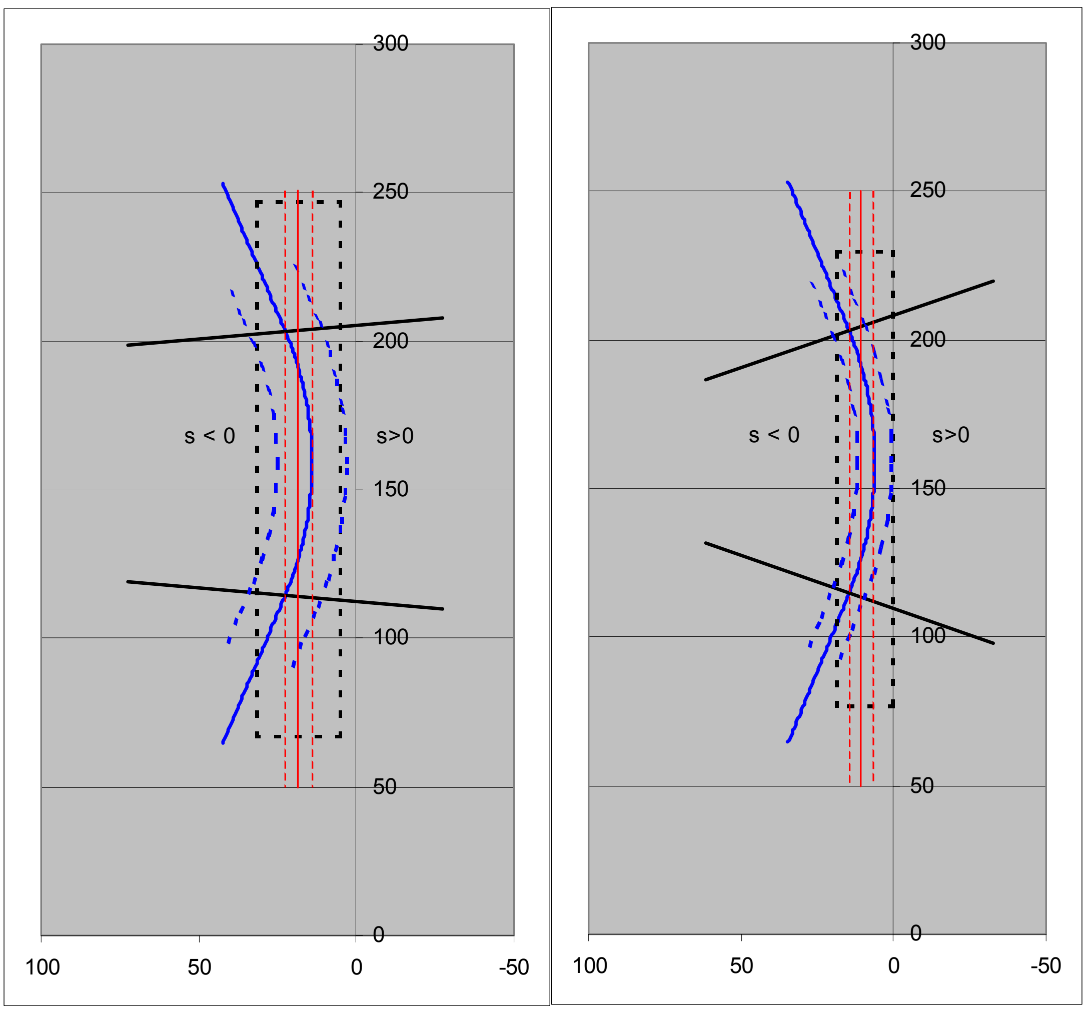

Figure 2: Revision of Figure 1 showing limits of measurement, working aperture, and Criterion 3 integration paths for GQ (left) and GX (right).

In the GQ, the test integration paths lie entirely within the working aperture (and thus the design good field), at least within the core of the magnet. In the GX, however, portions of the paths along the DIMAD chord and the tangent chord (dashed lines) are outside the working aperture, even inside the magnet. Therefore, Criterion 3 may not be met, inasmuch as the field variation may exceed specification in some of the regions that are sampled. We note that for the GX, even the half-sagitta line lies barely (at best!) within the working aperture inside the magnet core (because of the large sagitta and relatively small working aperture). Transverse field integral uniformity at the 10^{-4} level can therefore, even optimistically, be expected only over a small region around the half sagitta line. A match to the expected design result within the specified tolerance over even a limited range around the half-sagitta line (for example, over ±1 cm) will thus more properly serve to certify that the magnet "wedge angle" is set correctly than will the "DIMAD chord to tangent cord" specification of Criterion 3.

Figure 3 shows deviations of the straight-through field integrals from design as a function of transverse offset from the half-sagitta line for, respectively, GQ001, GQ002, GX001 and GX003 at 145 MeV/c (right) and 80 MeV/c (left). The sagitta is ~8.5 cm, so the DIMAD chord is at ~4.25 cm and the tangent chord at –4.25 cm. The GQ results clearly meet Criterion 3. The GX results do not; the variation exceeds 10^{-4} by a factor of two or so. Given the above discussion, we do however conclude the *intent* of Criterion 3 – namely, certification of the bend wedge angle – is satisfied.

Core field and field integral offsets of ~0.4% at low excitation – discussed above – are seen in these data as well. The transverse variation in integral is, as expected, greater for the GX. Further insight as to the source of this variation is provided by Figure 4, wherein the field is plotted as a function of distance along various straight-line paths through one of each of the dipoles at the excitation appropriate for 145 MeV/c. As the paths traverse larger portions of the "bad field" regions in the GX, this variation is much greater, and, as a consequence, the integrals along these paths exhibit greater variability as well.

Figure 3: Straight through field integrals as function of offset from half-sagitta line.

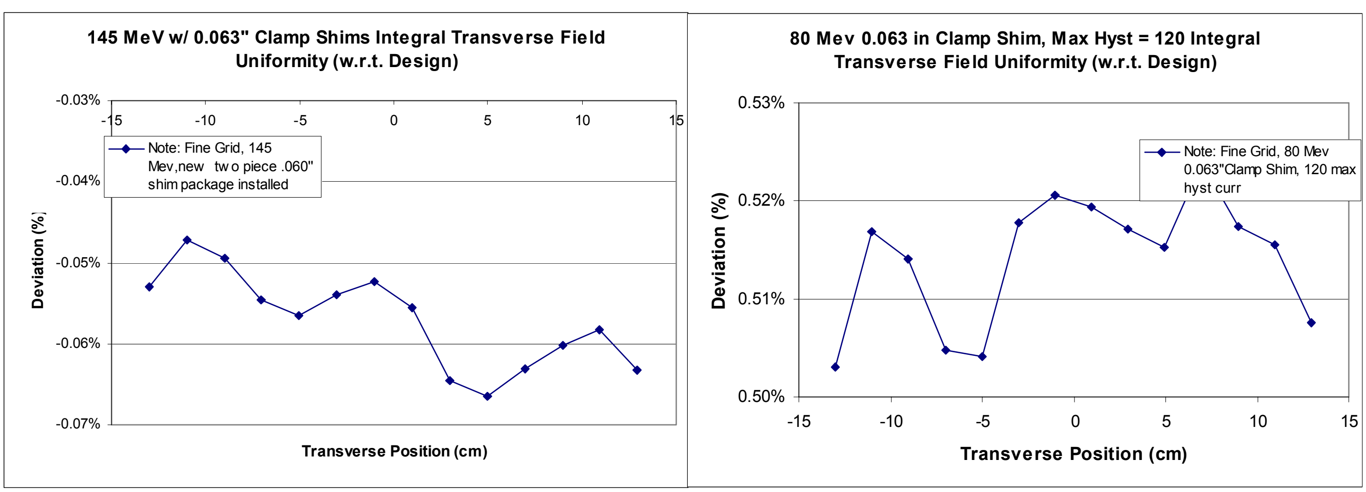

Figure 3a: GQ001 at 145 MeV/c (left) and 80 MeV/c (right).

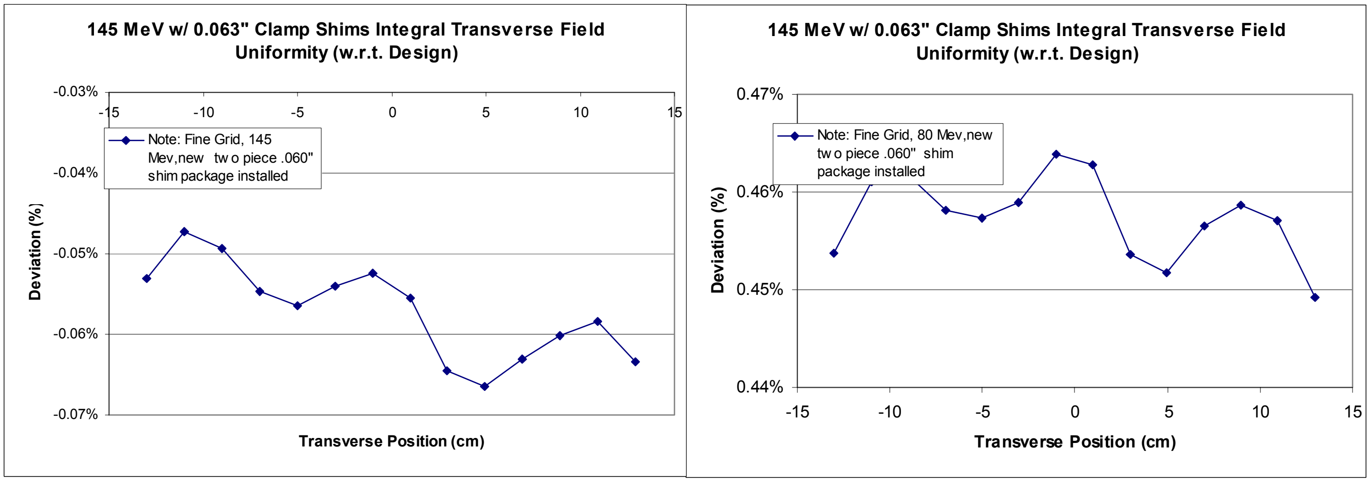

Figure 3b: GQ002 at 145 MeV/c (left) and 80 MeV/c (right).

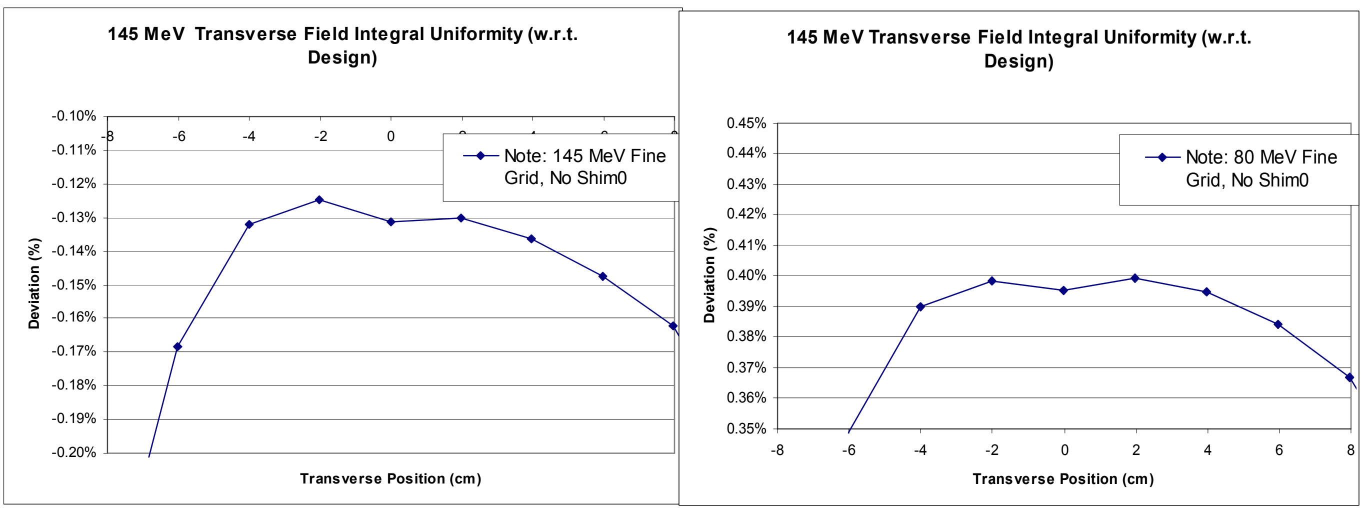

Figure 3c: GX001 at 145 MeV/c (left) and 80 MeV/c (right).

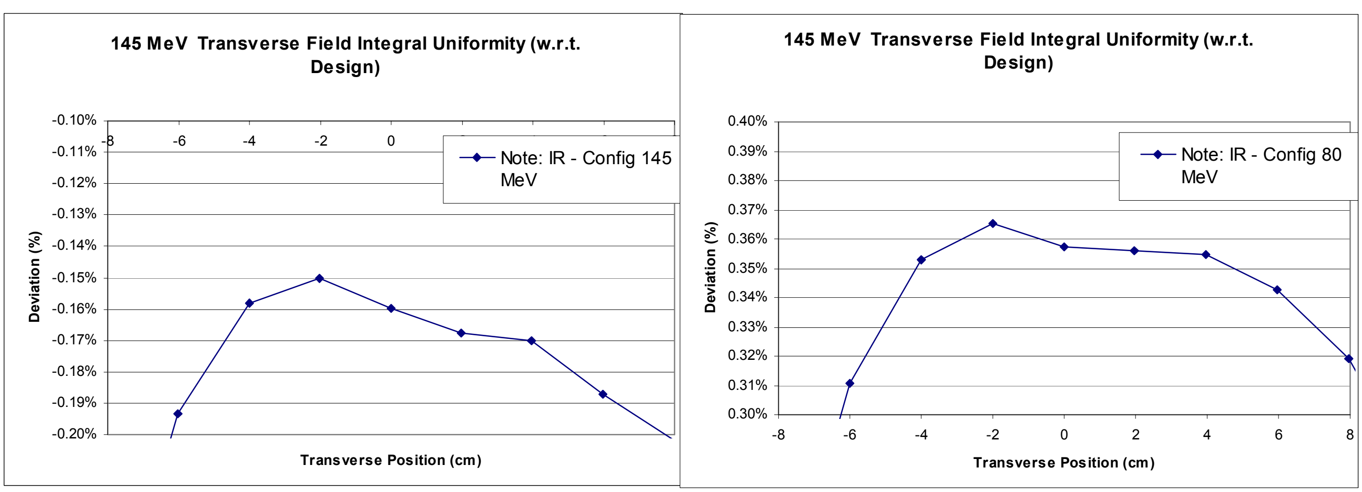

Figure 3d: GX003 at 145 MeV/c (left) and 80 MeV/c (right).

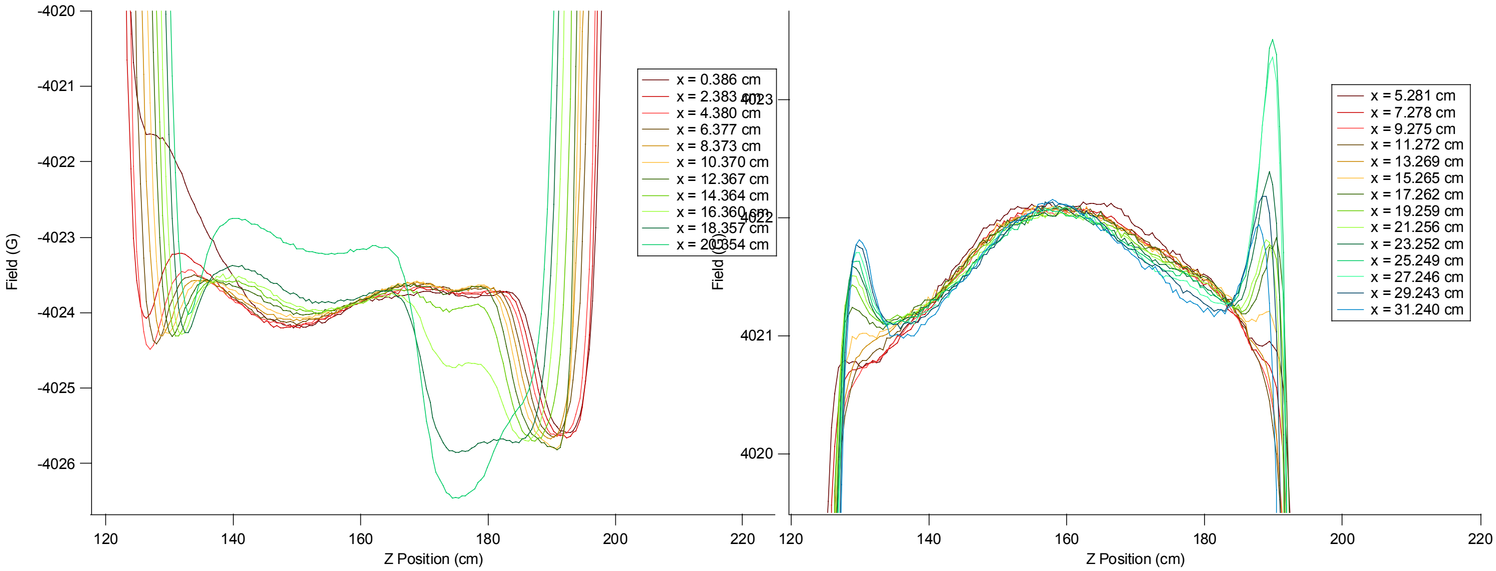

Figure 4: Longitudinal field profiles at different transverse offsets from the half-sagitta line in GX (left) and GQ (right) when excited for 145 MeV/c operation.

Criterion 4: Figure 5 presents contour maps of each dipole at each excitation. They are nonpathological and suggest the field will be flat to 0.1‰ over the entire working aperture. An earlier note evaluated the design performance of these dipoles [4]. Figure 6 compares the measured performance of GX003 (Figure 5g with a different orientation) with the design calculation [5]. The agreement is reassuring. We note that the scalloping at the plot edges is an artifact of graphing gridded data.

Criterion 5: Figure 7 presents plots of field vs. displacement transverse to the design orbit for each dipole at both 80 and 145 MeV/c. The data correspond to the transverse lines displayed in Figure 1. In each case, we provide the full range of available data (left) and, on expanded scale, zoom in on the core data (right). The flatness of the core data is apparent, indicating that the magnets meet the desired 0.1‰ tolerance across the working aperture. Key to an understanding of beam performance in such magnets is the awareness that it is *transverse* variation that is of importance – longitudinal variations (such as those shown in Figure 4) will average out along the magnet, provided that they are systematically uniform transversely.

Figure 5: Contour maps of GX and GQ performance

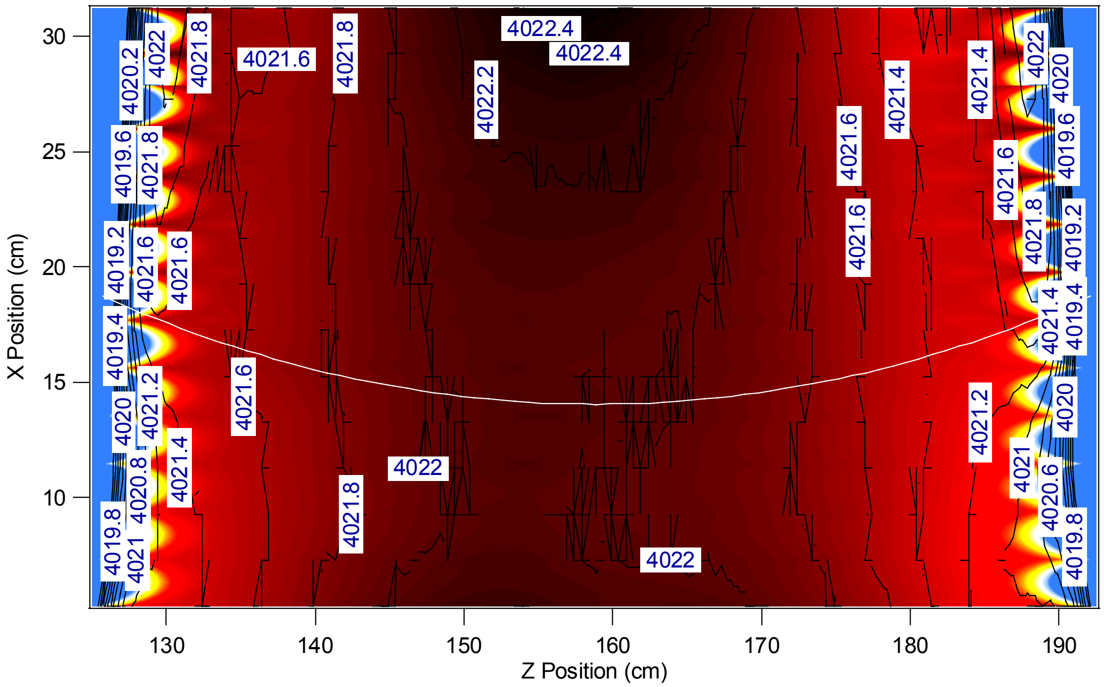

Figure 5a: GQ001 at 145 MeV/c

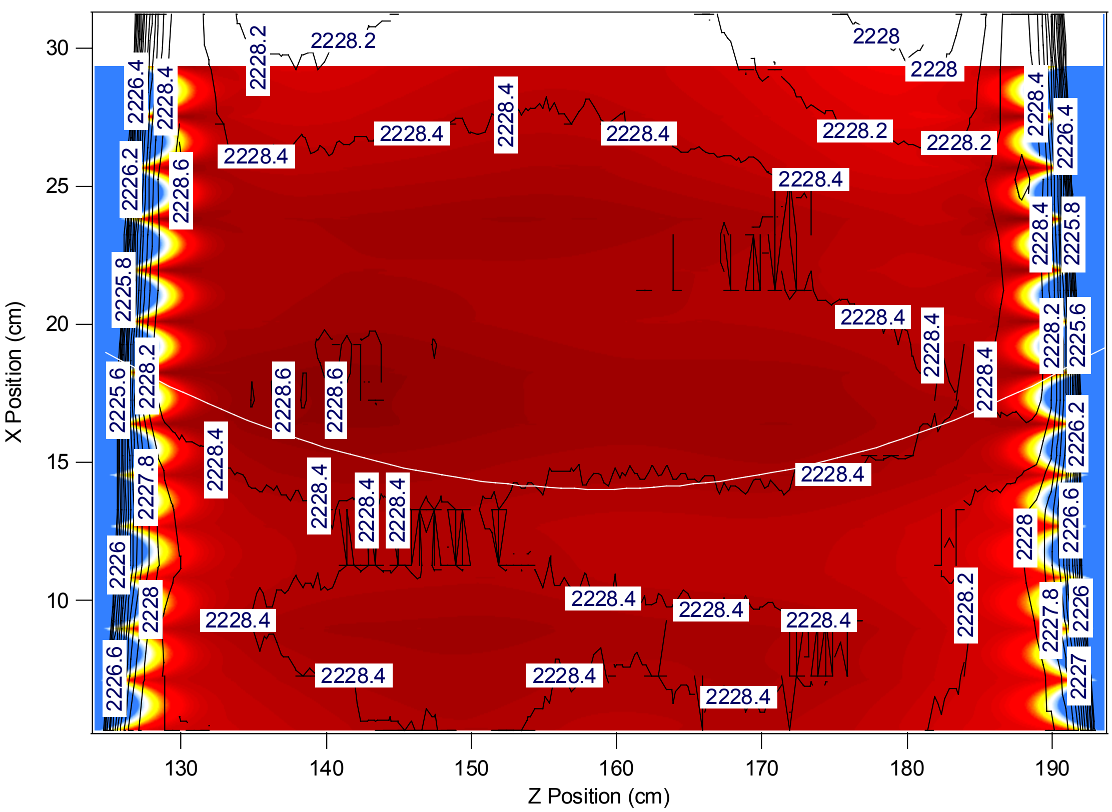

Figure 5b: GQ001 at 80 MeV/c

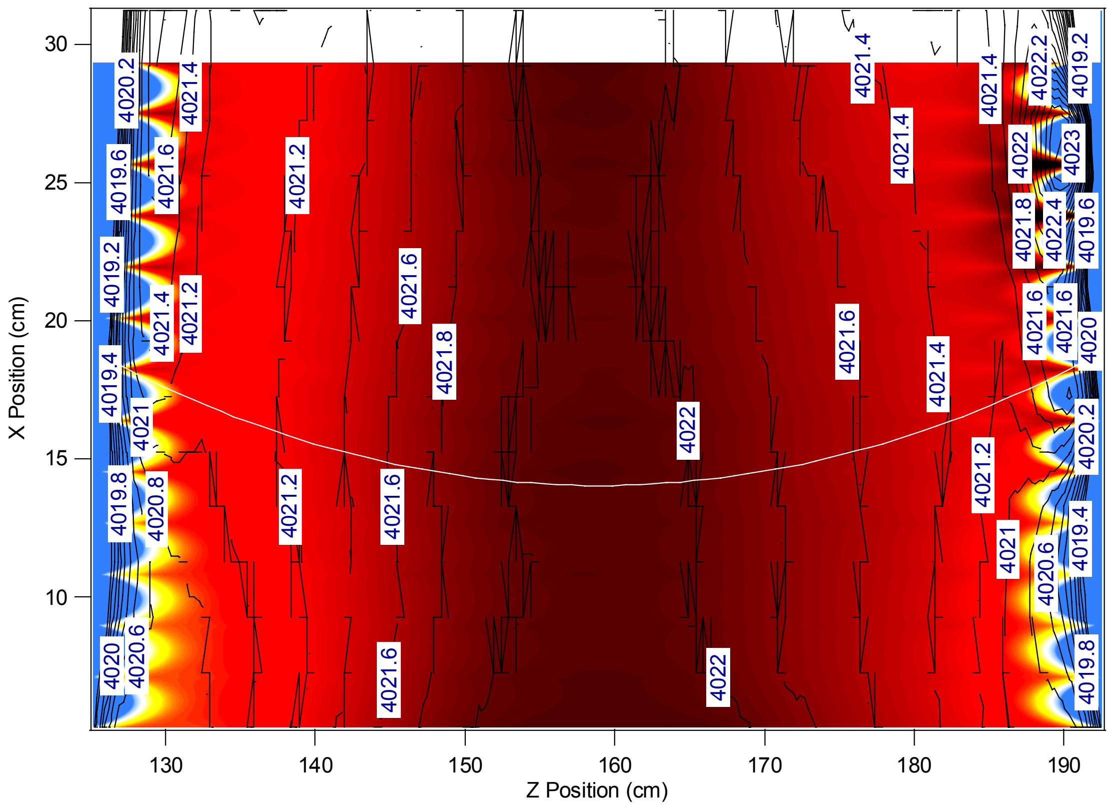

Figure 5c: GQ002 at 145 MeV/c

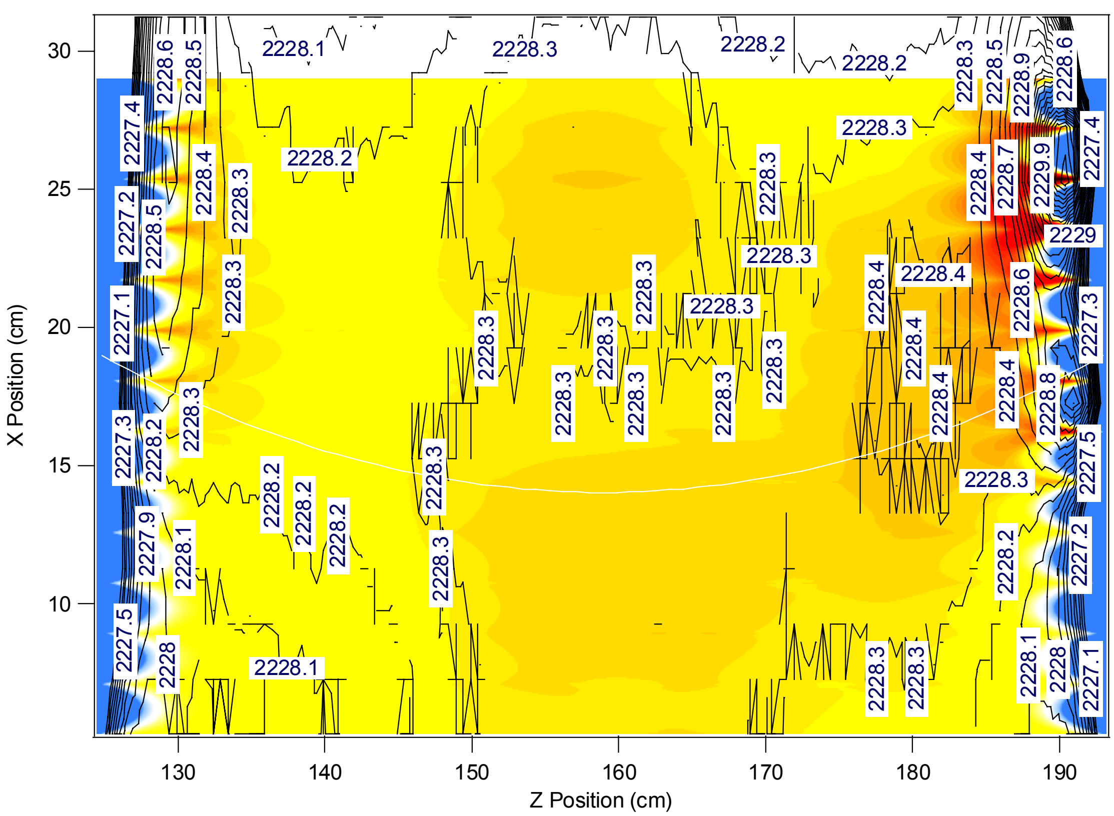

Figure 5d: GQ002 at 80 MeV/c

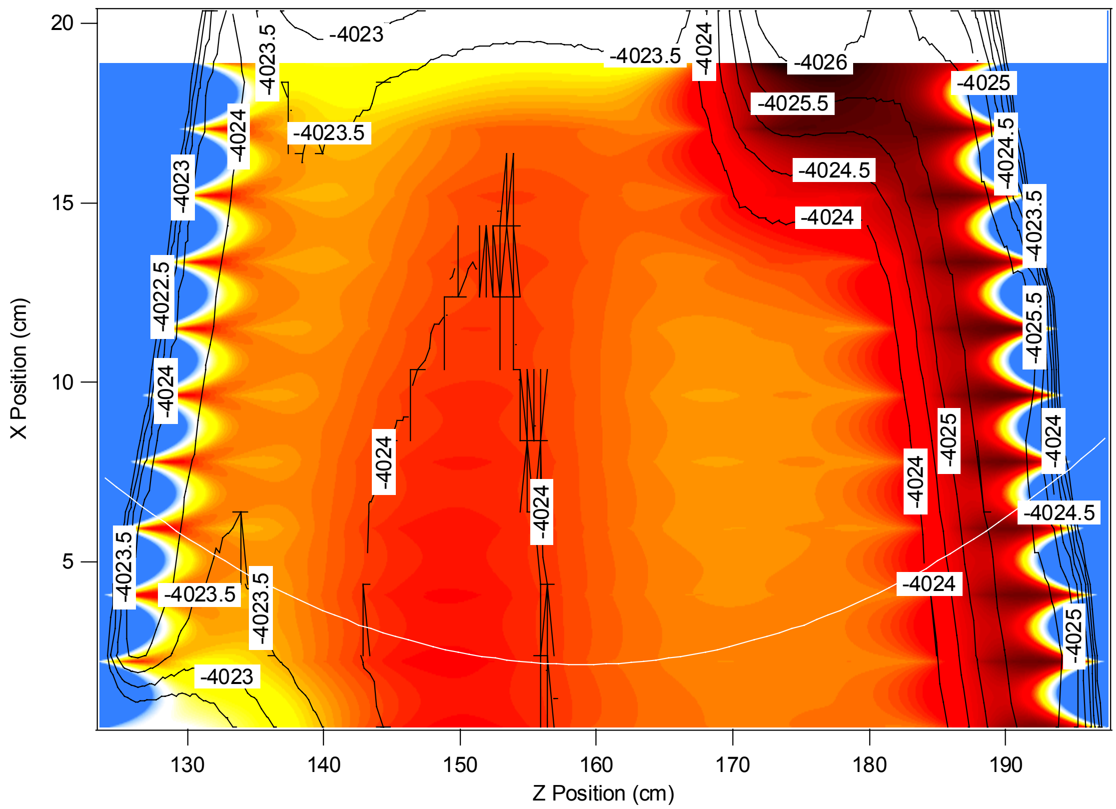

Figure 5e: GX001 at 145 MeV/c

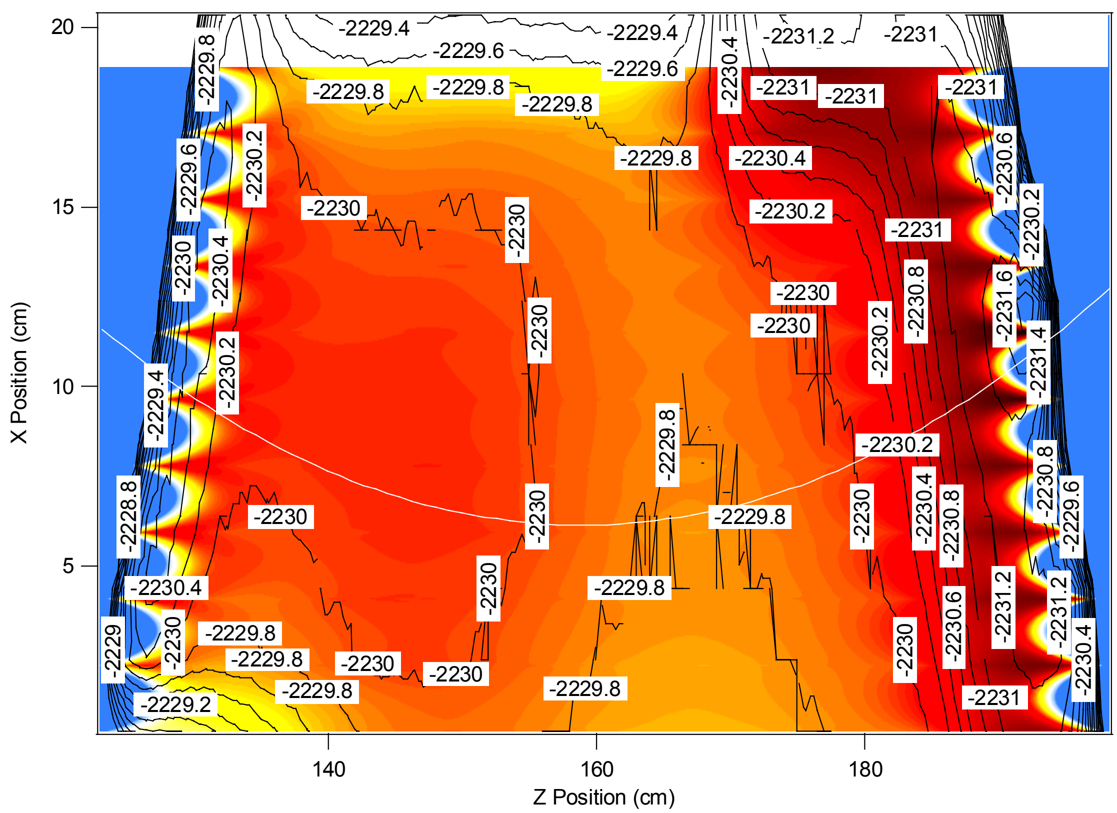

Figure 5f: GX001 at 80 MeV/c

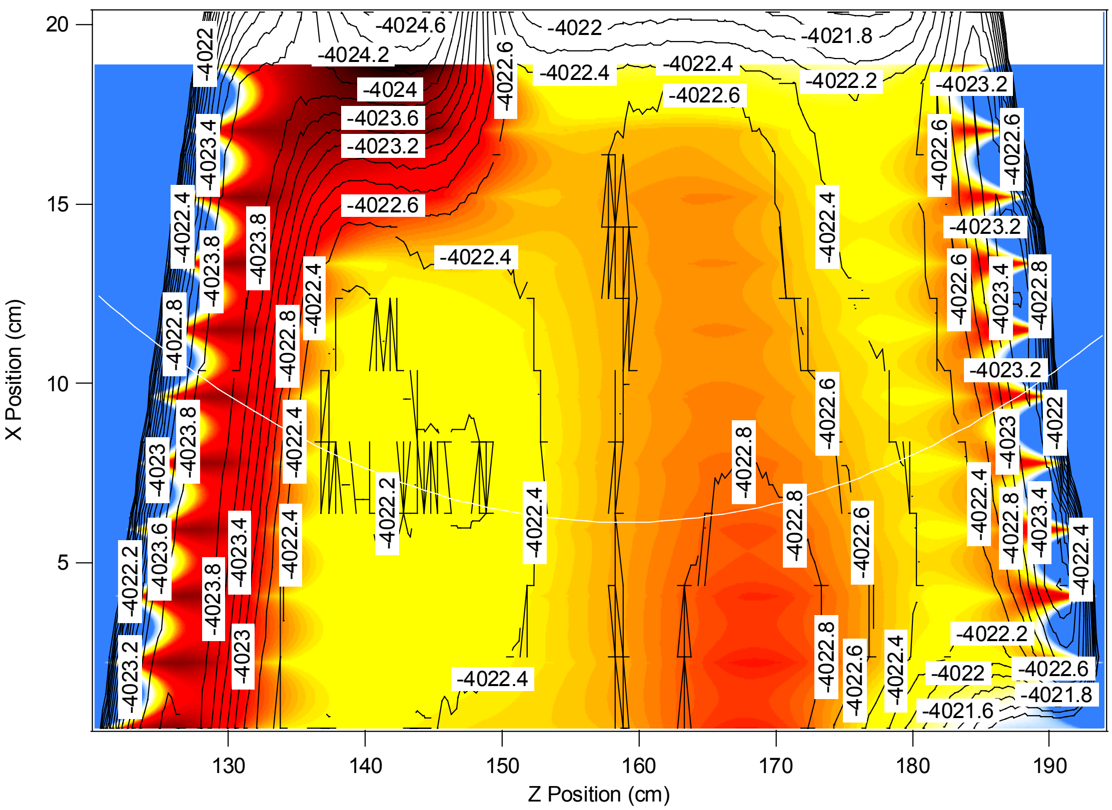

Figure 5g: GX003 at 145 MeV/c

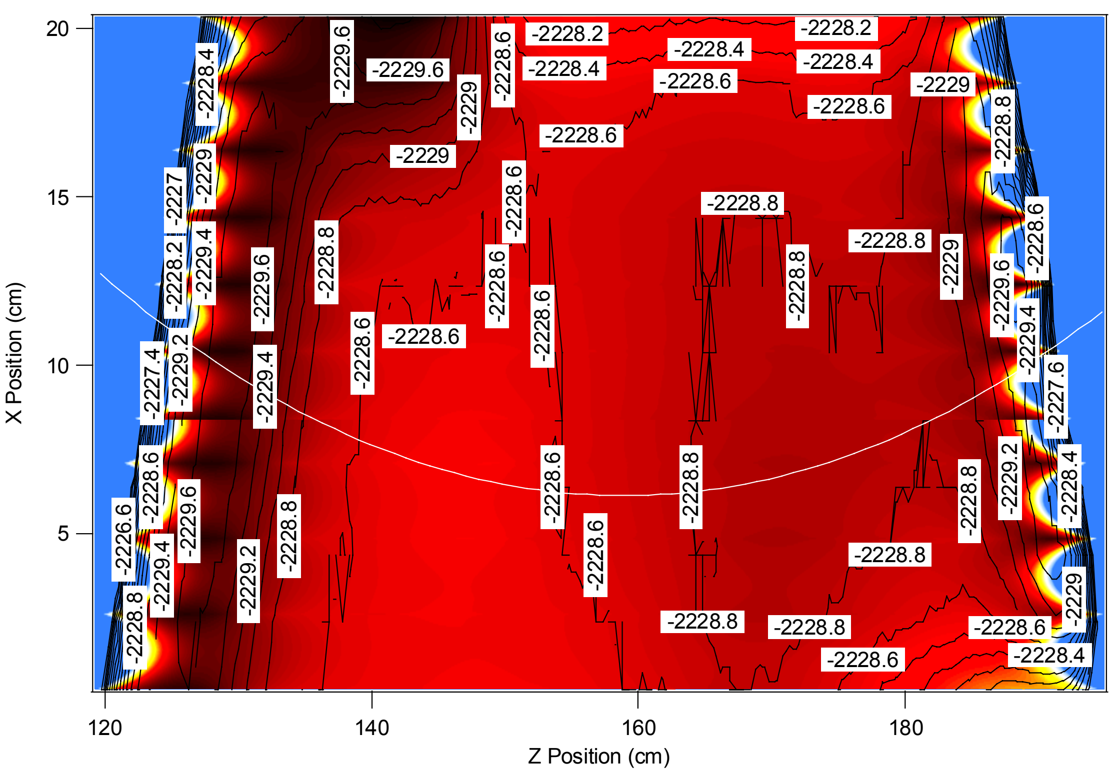

Figure 5h: GX003 at 80 MeV/c

Figure 6: Comparison of GX003 data and GX design prediction

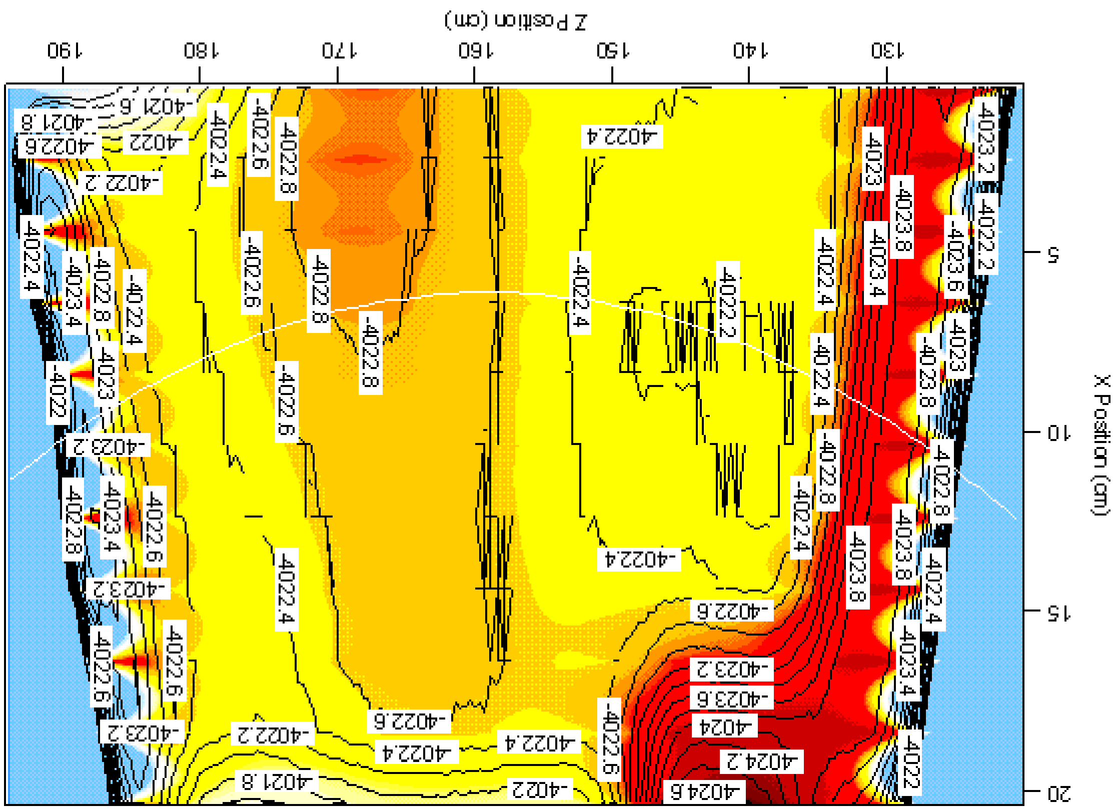

Figure 6a: Measured data, GX003 at 145 MeV/c (Figure 5g with different orientation).

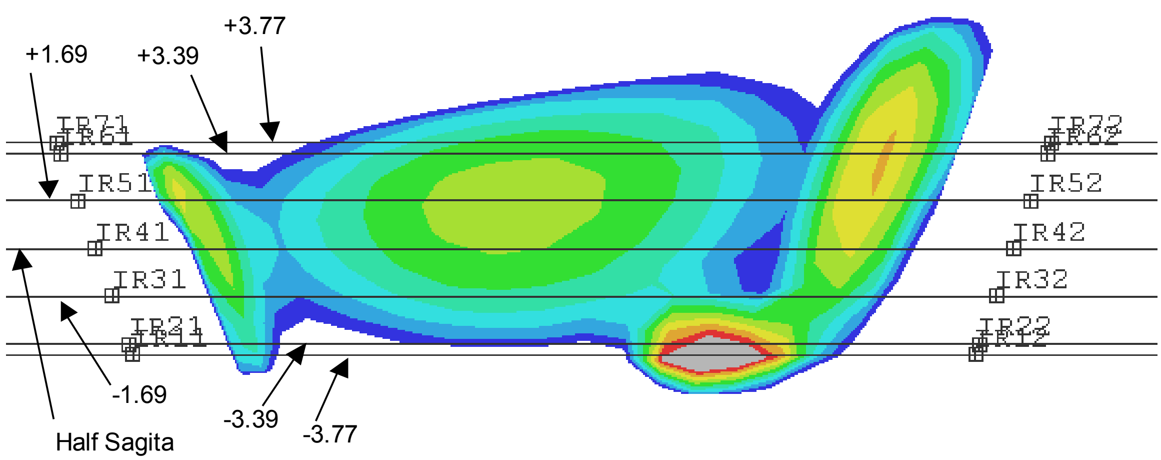

Figure 6b: GX design computation [5].

Figure 7: Field in dipoles vs. transverse position at locations along deign orbit, as shown in Figure 1.

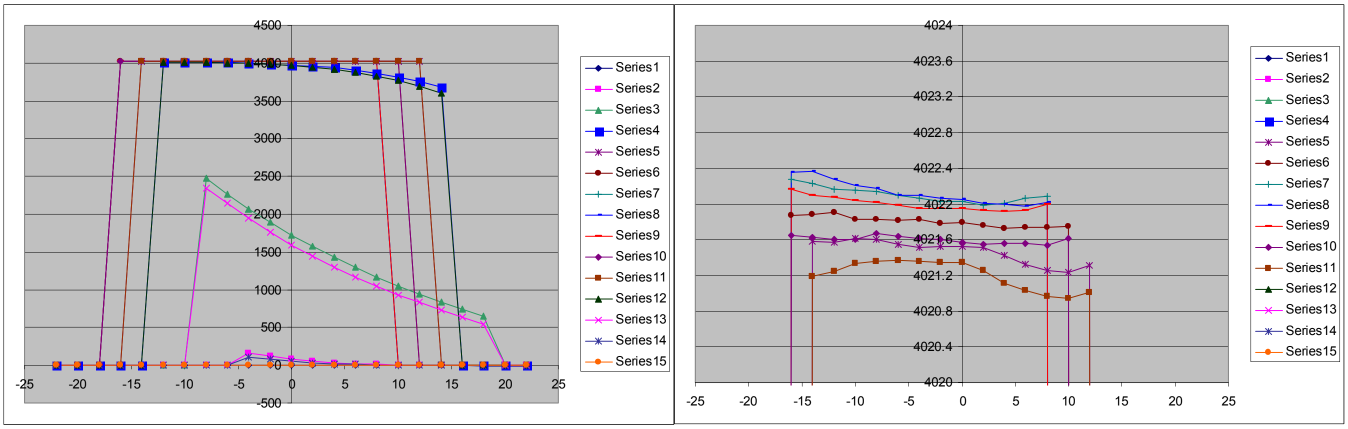

Figure 7a: GQ001 at 145 MeV/c

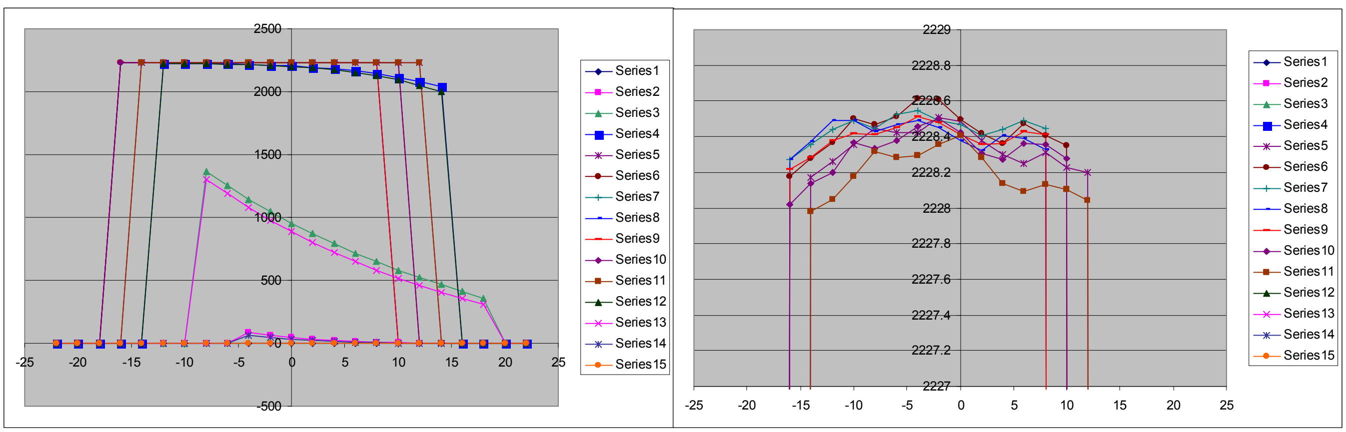

Figure 7b GQ001 at 80V/c

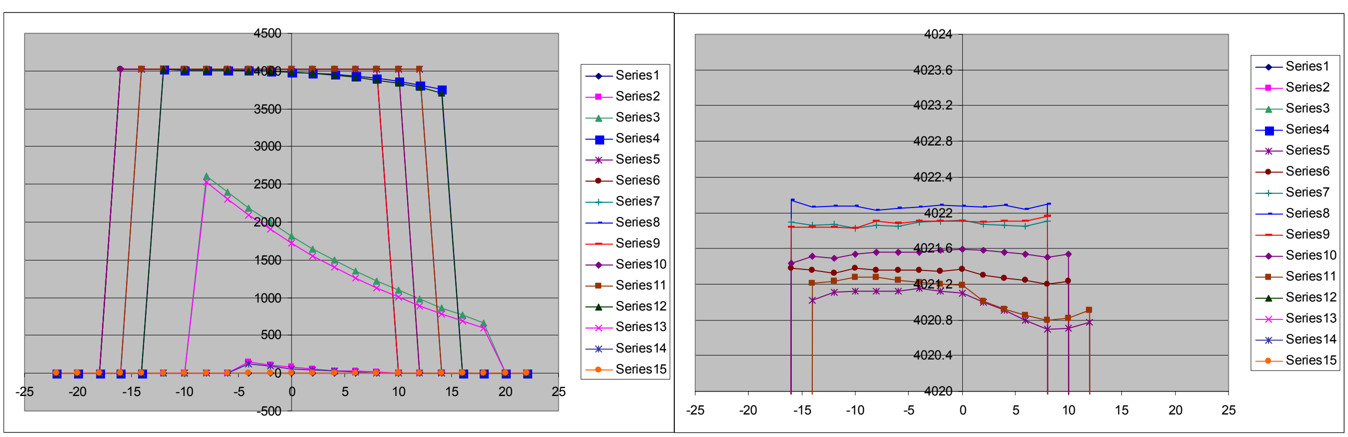

Figure 7c: GQ002 at 145 MeV/c

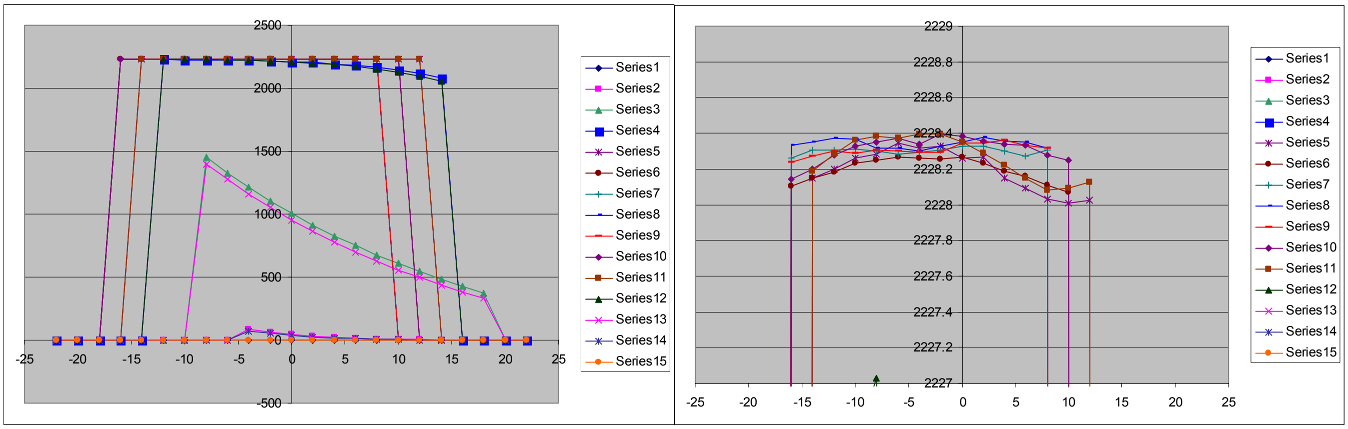

Figure 7d: GQ002 at 80 MeV/c

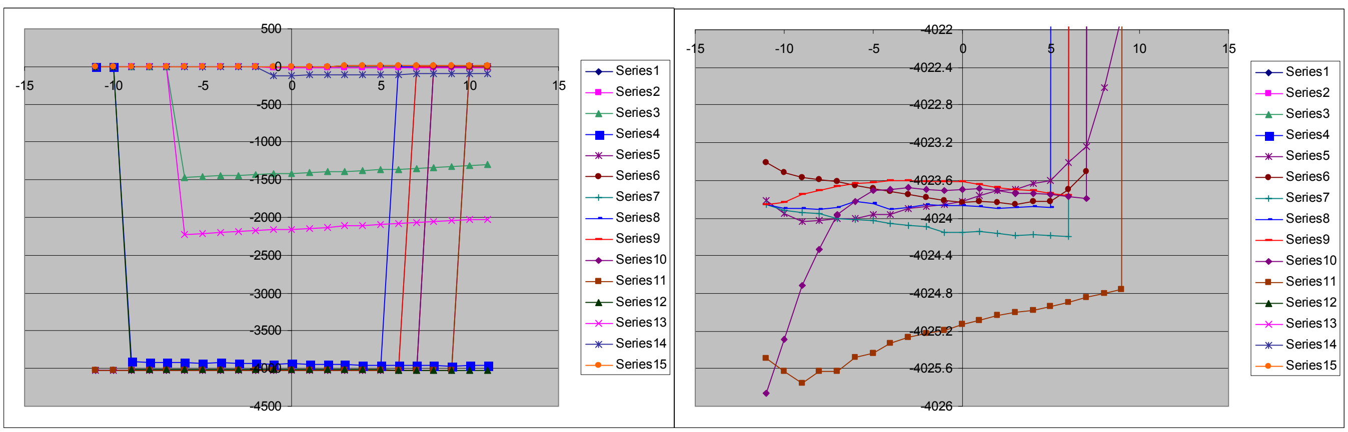

Figure 7e: GX001 at 145 MeV/c

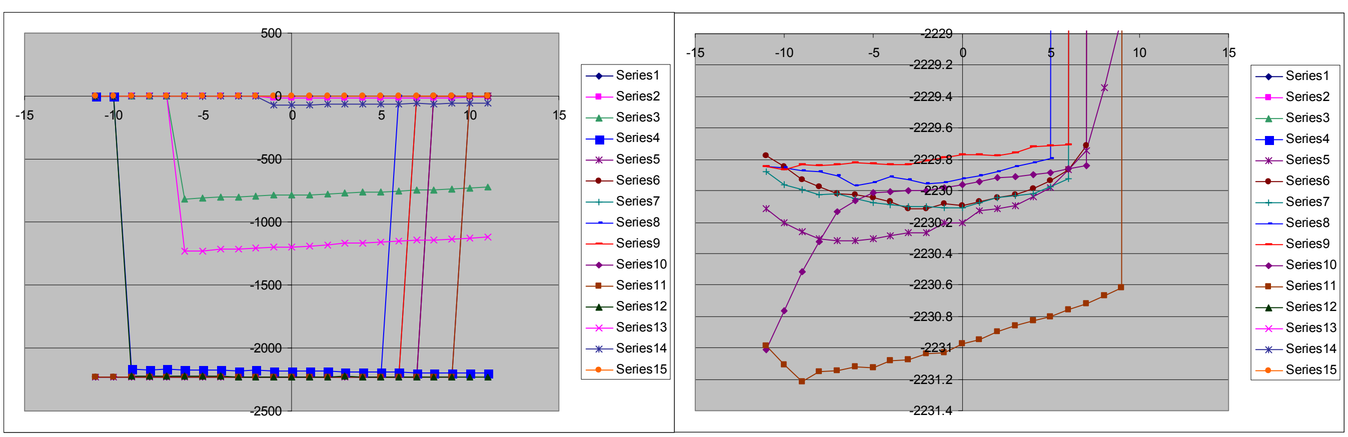

Figure 7f: GX001 at 80 MeV/c

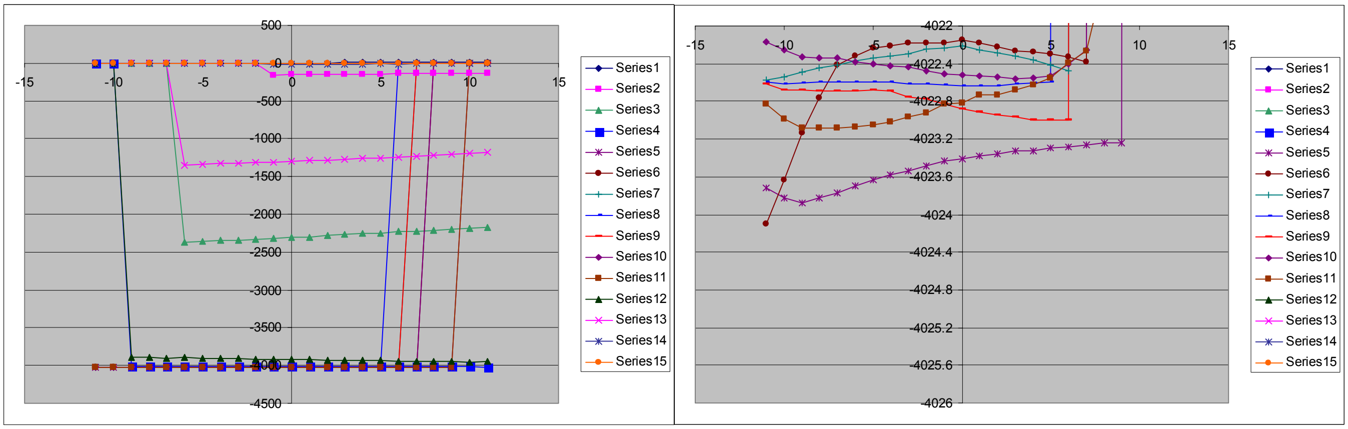

Figure 7g: GX003 at 145 MeV/c

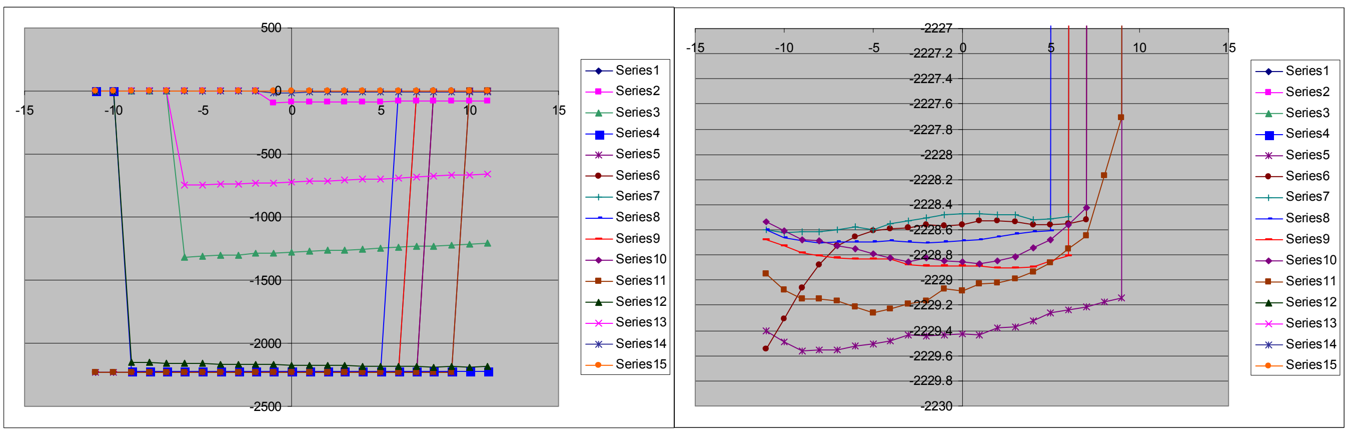

Figure 7h: GX003 at 80 MeV/c

Conclusions and Comments

Magnetic measurements have demonstrated that the GX and GQ dipoles installed in the FEL Upgrade 2F recirculation arc meet specification in all relevant areas. Field and field integral values track amongst and across families to the desired 1‰. Field and field integrals were found to be systematically shifted from the anticipated (design) values at 80 MeV/c; this can however be compensated by a commensurate shift in the 2F dipole buss excitation and, if needed, an appropriate associated offset of the GY shunt setting. Straight through field integrals matched the design central value and linear variation (to the specified 0.1‰, after appropriate adjustment of field clamp position), verifying the dipole effective length and wedge angles are correct. Contour plots of the field maps and various views of field variation with the transverse and longitudinal position demonstrate the 0.1‰ field homogeneity specification is satisfied throughout the working aperture.

These measurements were carried out on excitation-range specific standardization loops. Measurements at 145 MeV/c were made on a 228 A hysteresis loop; 80 MeV/c measurements were made on a 120 A hysteresis loop.

The preceding discussion assumed that installation of the vacuum chamber would lead to a systematic field enhancement of ~0.2% in all magnets. Work progressing in parallel to this analysis has determined that the chamber-induced enhancement is in fact greater in magnitude, and varies from chamber to chamber [6]. A simple average of all data presented in Table 2 of reference [6] suggests that the chambers will provide an average enhancement of ~0.34%, with a standard deviation of ~0.05%. The field variation within and between families may therefore be viewed as a systematic offset of ~1/3%, with individual magnet-to-magnet variations falling within the 0.1% tolerance discussed above. This, together with the palliative measures discussed in the reference (such as adding additional steel to jacket thinner chambers and thereby adjust the field enhancement factor), suggests that chamber-induced variations in field will not drive magnet performance outside the specified tolerances.

References

[1] D. Douglas, "Error Estimates for the IR FEL Transport System", CEBAF-TN-96-035, 15 July 1996; D. Douglas and G. Biallas, "DC Field Quality Characterization of FEL Upgrade Dipoles", JLAB-TN-02-041, 24 September 2002.

[2] D. Douglas, "IR Upgrade Driver Design, Revision 1.1.2", JLAB-TN-01-051, 26 October 2001.

[3] T. Hiatt *et al.*, "Magnet Measurements of the 10 kW, IR FEL Dipole Magnets" to appear in the Proceeding of PAC 2003.

[4] D. Douglas and G. Biallas, *op. cit.*

[5] T. Schultheiss, "GX Magnet Configuration wider evaluation lines 210 MeV/c IR", unpublished report, 2/6/01.

[6] T. Hiatt, M. Beck, G. Biallas, K. Sullivan, and D. Waldman, "Vacuum Chamber Contributions to 10 kW FEL Dipole Field Maps", JLAB-TN-03-007, 17 March 2003.